

# Stochastic Lagrangian models of velocity in homogeneous turbulent shear flow

Stephen B. Pope

*Department of Mechanical & Aerospace Engineering, Cornell University, Ithaca, New York 14853*

(Received 5 November 2001; accepted 31 January 2002; published 1 April 2002)

Stochastic Lagrangian models for the velocity following a fluid particle are used both in studies of turbulent dispersion and in probability density function (PDF) modeling of turbulent flows. A general linear model is examined for the important case of homogeneous turbulent shear flow, for which there are recent direct numerical simulation (DNS) data on Lagrangian statistics. The model is defined by a drift coefficient tensor and a diffusion tensor, and it is shown that these are uniquely determined by the normalized Reynolds-stress and timescale tensors determined from DNS. With the coefficients thus determined, the model yields autocorrelation functions in good agreement with the DNS data. It is found that the diffusion tensor is significantly anisotropic—contrary to the Kolmogorov hypotheses and conventional modeling—which may be a low-Reynolds-number effect. The performance of two PDF models is also compared to the DNS data. These are the simplified Lagrangian model and the Lagrangian isotropization of production model. There are significant differences between the autocorrelation functions generated by these models and the DNS data.

© 2002 American Institute of Physics. [DOI: 10.1063/1.1465421]

## I. INTRODUCTION

Homogeneous turbulent shear flow is of fundamental importance in the development of models for inhomogeneous turbulent flows. Both experiments<sup>1</sup> and direct numerical simulations (DNS)<sup>2</sup> of homogeneous shear flow have been performed in which Eulerian statistics of the turbulence have been measured. More recently, a series of DNS studies has been performed<sup>3–5</sup> in which Lagrangian statistics have been obtained by tracking a large number of fluid particles. These studies clearly have direct relevance to stochastic Lagrangian models<sup>6</sup> of turbulence, which model the motion of fluid particles as diffusion processes (i.e., continuous Markov processes).<sup>7</sup> The purpose of this paper is to show the connection between the Lagrangian velocity autocovariance tensor obtained from DNS and stochastic Lagrangian models for fluid particle velocity.

Stochastic Lagrangian models for the velocity of a fluid particle arise in two different contexts: turbulent dispersion;<sup>8–10</sup> and probability density function (PDF) models.<sup>11,12,7</sup> In both cases the general form of the models considered (when applied to homogeneous turbulence) can be written as the linear stochastic differential equation (SDE)

$$du_i = -A_{ij}u_j dt + B_{ij}dW_j, \quad (1)$$

where  $d\mathbf{u}(t) \equiv \mathbf{u}(t+dt) - \mathbf{u}(t)$  is the infinitesimal increment of the fluctuating component of velocity  $\mathbf{u}(t)$  following the fluid particle; we refer to  $\mathbf{A}(t)$  as the drift tensor;  $\mathbf{B}(t)$  is the diffusion coefficient; and  $d\mathbf{W}(t)$  is the infinitesimal increment of a vector-valued Wiener process which has the properties  $\langle d\mathbf{W} \rangle = 0$ ,  $\langle dW_i dW_j \rangle = dt \delta_{ij}$ . Different models correspond to different specifications of the drift tensor  $\mathbf{A}(t)$  and diffusion coefficient  $\mathbf{B}(t)$ .

For statistically stationary, homogeneous isotropic turbulence (with no mean velocity gradients) the only sensible choice of coefficients is

$$A_{ij} = \frac{\delta_{ij}}{T_L}, \quad (2)$$

and

$$B_{ij} = \left( \frac{2u'^2}{T_L} \right)^{1/2} \delta_{ij}, \quad (3)$$

where  $T_L$  is the Lagrangian integral timescale and  $u'$  is the turbulence intensity (i.e., the rms velocity fluctuation). Then, Eq. (1) reduces to an independent Langevin equation for each component of velocity

$$du_i = -u_i \frac{dt}{T_L} + \left( \frac{2u'^2}{T_L} \right)^{1/2} dW_i. \quad (4)$$

This model dates back to Taylor's 1921 original paper on turbulent dispersion.<sup>8</sup> The autocorrelation function given by Eq. (4) is

$$\rho(s) \equiv \langle u_1(t)u_1(t+s) \rangle / u'^2 = \exp(-|s|/T_L), \quad (5)$$

which agrees well with DNS data<sup>13</sup> (except at small values of  $|s|/T_L$ ).

The central issue addressed here is the appropriate specification of  $\mathbf{A}$  and  $\mathbf{B}$  in homogeneous turbulent shear flow. This has been considered in the context of turbulent dispersion by Sawford and Yeung.<sup>4,5</sup> These authors compared Lagrangian autocorrelations predicted by two dispersion models to DNS data. Both of these models take  $\mathbf{B}$  to be isotropic.

We show here that appropriate values of  $\mathbf{A}$  and  $\mathbf{B}$  can be deduced from the measured Lagrangian velocity autocovariance, and that the resulting model is in good agreement with

the DNS data. This agreement supports the nontrivial conclusion that the Lagrangian velocity is well represented by a linear diffusion process (except over small time intervals). The deduced value of  $\mathbf{B}$  is significantly anisotropic.

The performance of two models used in PDF methods is compared to the DNS data. These are the simplified Langevin model (SLM) and the Lagrangian isotropization of production (LIPM) model.<sup>14</sup>

## II. HOMOGENEOUS TURBULENT SHEAR FLOW

In homogeneous turbulent shear flow, the imposed mean velocity gradient is

$$\frac{\partial \langle U_i \rangle}{\partial x_j} = S \delta_{i1} \delta_{j2}, \quad (6)$$

where  $S$  is the (constant) imposed mean shear rate. The turbulence is characterized by the Reynolds stress tensor  $\langle u_i u_j \rangle$ , the turbulent kinetic energy  $k \equiv \frac{1}{2} \langle u_i u_i \rangle$ , and the mean dissipation rate  $\varepsilon$ . All of these quantities are uniform in space and evolve in time.

An essential observation from experiments and DNS is that, after an initial transient, the turbulence tends to an approximately self-similar state. The normalized Reynolds-stress tensor

$$C_{ij} \equiv \frac{\langle u_i u_j \rangle}{k} \quad (7)$$

becomes constant, as does the ratio of turbulence-to-shear timescales,  $Sk/\varepsilon$ , and hence also the ratio of production  $\mathcal{P}$  to dissipation  $\varepsilon$ . The turbulent kinetic energy equation then dictates that  $k$  and  $\varepsilon$  increase exponentially with time—as is observed. Thus when normalized by  $k$  and  $\varepsilon$ , quantities pertaining to the energy-containing scales of the turbulence are self-similar. Since the Reynolds number  $k^2/(\varepsilon \nu)$  increases with time, small-scale quantities are not self-similar under this scaling.

The DNS of Sawford and Yeung<sup>4,5</sup> are performed from the nondimensional time  $St=0$  until  $St=20$ . The fluid particles are introduced at  $St=4$  when the self-similar state has been attained. The values  $Sk/\varepsilon=4.83$  and  $\mathcal{P}/\varepsilon=1.54$  are deduced from the values of  $k$  and  $\langle u_1 u_2 \rangle$  from  $St=4$  until  $St=20$ ; and the average value of the normalized Reynolds stress tensor over this time interval is

$$\mathbf{C} = \begin{bmatrix} 0.96 & -0.32 & 0 \\ -0.32 & 0.43 & 0 \\ 0 & 0 & 0.61 \end{bmatrix}. \quad (8)$$

We introduce the normalized time

$$\hat{t} = t \frac{\varepsilon}{k}, \quad (9)$$

and the scaled fluctuating velocity following a fluid particle

$$\hat{\mathbf{u}}(\hat{t}) \equiv \frac{\mathbf{u}(t)}{k(t)^{1/2}}. \quad (10)$$

Consistent with the self-similar state of the turbulence, we assume that  $\hat{\mathbf{u}}(\hat{t})$  is a statistically stationary process.

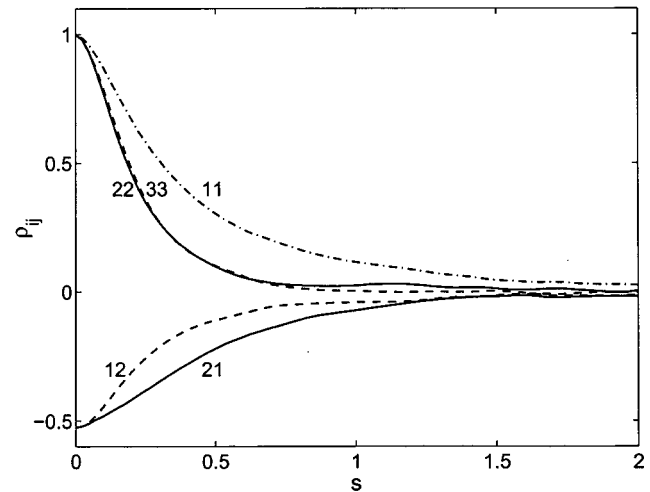


FIG. 1. Autocorrelation functions  $\rho_{ij}(s)$ , Eq. (14), from the DNS data of Sawford and Yeung (Ref. 5).

The autocovariance of  $\hat{\mathbf{u}}(\hat{t})$  is

$$\hat{R}_{ij}(s) \equiv \langle \hat{u}_i(\hat{t}) \hat{u}_j(\hat{t}+s) \rangle, \quad (11)$$

which (in view of the assumed stationarity) is independent of  $\hat{t}$ ; and the scaled Reynolds stress is

$$\langle \hat{u}_i(t) \hat{u}_j(t) \rangle = C_{ij} = \hat{R}_{ij}(0) = \frac{\langle u_i u_j \rangle}{k}, \quad (12)$$

which is constant. Note that (unlike  $C_{ij}$ )  $\hat{R}_{ij}(s)$  is not symmetric, although it has the property

$$\hat{R}_{ij}(s) = \hat{R}_{ji}(-s). \quad (13)$$

It is conventional to define autocorrelation functions by

$$\rho_{ij}(s) \equiv \frac{\hat{R}_{ij}(s)}{[C_{(i)(i)} C_{(j)(j)}]^{1/2}} \quad (14)$$

(where bracketed suffixes are excluded from the summation convention) so that the diagonal components of  $\rho_{ij}(0)$  are unity. These autocorrelation functions obtained from the DNS are shown in Fig. 1. (Note that, by symmetry,  $\rho_{23} = \rho_{32} = 0$ .)

The analysis below shows that a preferable definition of the autocorrelations is

$$R_{ij}(s) \equiv C_{ik}^{-1} \hat{R}_{kj}(s), \quad (15)$$

where  $C_{ik}^{-1}$  denotes the  $i-k$  component of the inverse of  $\mathbf{C}$ . Unlike  $\rho_{ij}$ ,  $R_{ij}$  is a tensor, and at the origin it is

$$R_{ij}(0) = \delta_{ij}. \quad (16)$$

These autocorrelation functions obtained from the DNS are shown in Fig. 2. [There is a small inconsistency in the extraction of numerical values from the DNS:  $C_{ij}$  is obtained as an average from  $St=4$  to  $St=20$ , whereas  $\hat{R}_{ij}(0)$  is obtained at  $St=4$ . As a consequence, as may be seen in Fig. 2, the numerical values do not satisfy Eq. (16) exactly.]

Based on  $R_{ij}(s)$ , we define the (normalized) integral timescales by

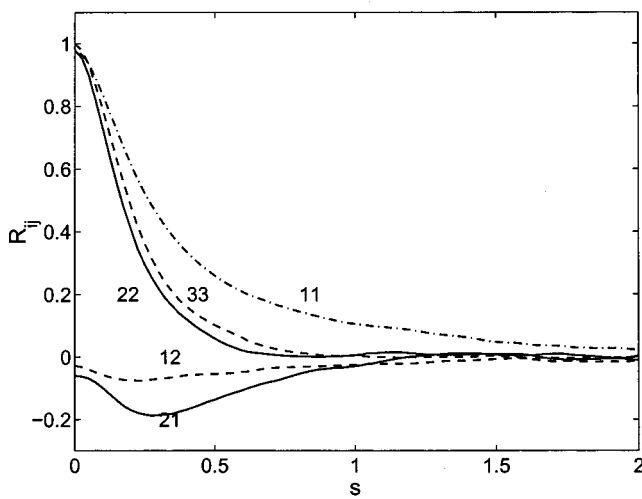


FIG. 2. Autocorrelation functions  $R_{ij}(s)$ , Eq. (15), from the DNS data of Sawford and Yeung (Ref. 5).

$$T_{ij} \equiv \int_0^\infty R_{ij}(s) ds. \quad (17)$$

The values deduced from the DNS data are

$$\mathbf{T} = \begin{bmatrix} 0.44 & -0.06 & 0 \\ -0.11 & 0.22 & 0 \\ 0 & 0 & 0.24 \end{bmatrix}. \quad (18)$$

### III. STOCHASTIC MODEL

The stochastic model considered is Eq. (1) written for  $\hat{\mathbf{u}}(\hat{t})$ . It is convenient to use matrix notation, and so the equation is written

$$d\hat{\mathbf{u}} = -\mathbf{A}\hat{\mathbf{u}} d\hat{t} + \mathbf{B} d\hat{\mathbf{W}}, \quad (19)$$

where  $\langle d\hat{\mathbf{W}} d\hat{\mathbf{W}}^T \rangle = \mathbf{I} dt$ , with  $\mathbf{I}$  being the identity, and  $T$  denoting the transpose.

The drift matrix  $\mathbf{A}$  is constant and it is required that its eigenvalues have positive real parts. The value of  $\mathbf{A}$  deduced from the DNS (below) has the simplest structure—real positive eigenvalues and independent eigenvectors. In this case  $\mathbf{A}$  can be decomposed as

$$\mathbf{A} = \mathbf{V} \Lambda \mathbf{V}^{-1}, \quad (20)$$

where the columns of  $\mathbf{V}$  are the eigenvectors of  $\mathbf{A}$ , and  $\Lambda$  is the diagonal matrix of eigenvalues.

The diffusion coefficient matrix  $\mathbf{B}$  is also constant and, without loss of generality,<sup>7</sup> we take it to be symmetric ( $\mathbf{B} = \mathbf{B}^T$ ).

#### A. Autocorrelation function

It is readily deduced from Eq. (19) that the autocovariance matrix  $\hat{\mathbf{R}}(s)$  [Eq. (11)] satisfies the ordinary differential equation

$$\frac{d\hat{\mathbf{R}}}{ds} = -\mathbf{A}\hat{\mathbf{R}}^T, \quad \text{for } s \geq 0. \quad (21)$$

By post-multiplying both sides of this equation by  $\mathbf{C}^{-1}$ , we find that  $\mathbf{R}(s)$  [defined by Eq. (15)] satisfies the same equation

$$\frac{d\mathbf{R}^T}{ds} = -\mathbf{A}\mathbf{R}^T, \quad \text{for } s \geq 0, \quad (22)$$

with the simple initial condition  $\mathbf{R}^T(0) = \mathbf{I}$ . The solution to this equation (satisfying the initial condition) is<sup>15</sup>

$$\mathbf{R}^T(s) = \exp(-\mathbf{As}) = \sum_{n=0}^{\infty} \frac{(-1)^n}{n!} \mathbf{A}^n s^n, \quad \text{for } s \geq 0, \quad (23)$$

as may be verified by differentiating with respect to  $s$ . It has been assumed that the eigenvalues of  $\mathbf{A}$  have positive real parts, which is a sufficient condition for  $\exp(-\mathbf{As})$  to converge to zero as  $s$  tends to infinity.

In the case that  $\mathbf{A}$  has linearly independent eigenvectors the solution can be written

$$\mathbf{R}^T(s) = \mathbf{V} \exp(-\Lambda s) \mathbf{V}^{-1}, \quad \text{for } s \geq 0, \quad (24)$$

and similarly for  $\hat{\mathbf{R}}$

$$\hat{\mathbf{R}}(s)^T = \mathbf{V} \exp(-\Lambda s) \mathbf{V}^{-1} \mathbf{C}, \quad \text{for } s \geq 0. \quad (25)$$

Thus each component of the autocovariance is a linear combination of three decaying exponentials—decaying because the eigenvalues are required to be positive.

For the autocorrelation timescales,  $\mathbf{T}$  [Eq. (17)] we obtain

$$\mathbf{T}^T \equiv \int_0^\infty \mathbf{R}^T(s) ds = \int_0^\infty \exp(-\mathbf{As}) ds = \mathbf{A}^{-1}. \quad (26)$$

The conclusion from this development is that the matrix of autocorrelation timescales  $\mathbf{T}$  of the process  $\hat{\mathbf{u}}(\hat{t})$  generated by the stochastic model Eq. (19) is uniquely determined by the drift matrix  $\mathbf{A}$  as

$$\mathbf{T} = (\mathbf{A}^{-1})^T. \quad (27)$$

This conclusion depends on the eigenvalues of  $\mathbf{A}$  having positive real parts.

#### B. Covariance

It follows from Eq. (19) that the covariance  $\mathbf{C} = \langle \hat{\mathbf{u}}\hat{\mathbf{u}}^T \rangle$  evolves by

$$\frac{d\mathbf{C}}{dt} = -\mathbf{AC} - \mathbf{CA}^T + \mathbf{BB}^T. \quad (28)$$

Given that  $\mathbf{B}$  is symmetric and that the process is stationary, this leads to the relation

$$\mathbf{B}^2 = \mathbf{AC} + \mathbf{CA}^T. \quad (29)$$

#### C. Specification of stochastic model coefficients

Can the model coefficients  $\mathbf{A}$  and  $\mathbf{B}$  be chosen so that the autocovariance  $\hat{\mathbf{R}}(s)$  from the model matches that obtained from DNS of homogeneous turbulent shear flow? Clearly the answer is “no,” since the empirical autocovariances will not be of the simple form implied by the model—i.e., sums of

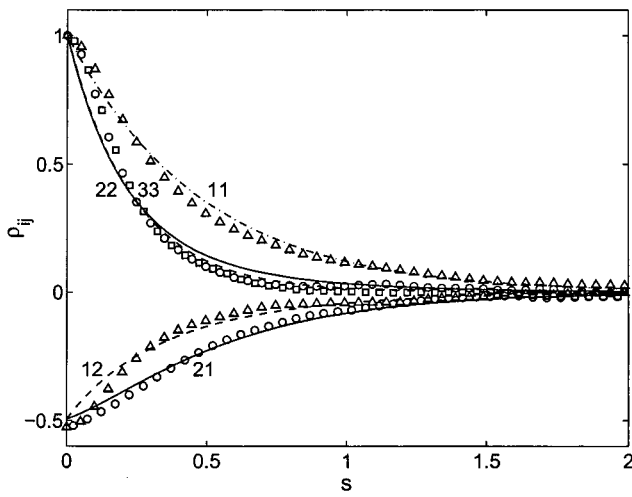


FIG. 3. Comparison of autocorrelation functions  $\rho_{ij}(s)$ , Eq. (14), from the DNS data (symbols) and from the stochastic model (lines) with coefficients determined from the data [Eq. (32) and Eq. (33)]. ( $\rho_{22}$  circles and solid line;  $\rho_{33}$  squares and dashed line.)

three exponentials. Nevertheless, the preceding analysis shows that  $\mathbf{A}$  and  $\mathbf{B}$  can be chosen to match the covariance  $\mathbf{C}$  and the timescales  $\mathbf{T}$ . Specifically, given  $\mathbf{T}$ ,  $\mathbf{A}$  is determined by

$$\mathbf{A} = (\mathbf{T}^{-1})^T \quad (30)$$

[see Eq. (27)]; then  $\mathbf{B}$  is determined as the symmetric square root of

$$\mathbf{B}^2 = \mathbf{AC} + \mathbf{CA}^T \quad (31)$$

[see Eq. (29)]. Evidently this specification requires that  $\mathbf{T}$  be nonsingular. An additional requirement is that  $\mathbf{T}$  and  $\mathbf{C}$  be such that  $\mathbf{B}^2$  given by Eq. (31) is positive semi-definite.

For the values of  $\mathbf{C}$  and  $\mathbf{T}$  obtained from the DNS of homogeneous turbulent shear flow, the values of  $\mathbf{A}$  and  $\mathbf{B}^2$  obtained from Eq. (30) and Eq. (31) are

$$\mathbf{A} = \begin{bmatrix} 2.45 & 1.24 & 0 \\ 0.65 & 4.90 & 0 \\ 0 & 0 & 4.22 \end{bmatrix}, \quad (32)$$

and

$$\mathbf{B}^2 = \begin{bmatrix} 3.90 & -1.18 & 0 \\ -1.18 & 3.84 & 0 \\ 0 & 0 & 5.14 \end{bmatrix}. \quad (33)$$

#### D. Comparison of autocorrelation functions

Figure 3 shows the comparison between the autocorrelation functions  $\rho_{ij}(s)$  obtained from DNS compared to those from the model [with coefficients given by Eq. (32) and Eq. (33)]. Inevitably there are qualitative differences at the origin. For  $\rho_{11}$ , for example, the DNS value departs from unity at the origin as  $1 - \rho_{11}(s) \sim s^2$ , whereas the model departs as  $1 - \rho_{11}(s) \sim |s|$ . This leads to the model values of  $\rho_{11}(s)$  being below the DNS values at small times; and then, from the matching of the integral timescales, it is not surprising

that at some later times the model value exceeds the DNS value. Given these inevitable differences, the agreement between the model and the DNS is as good as could be expected. In particular the model captures the difference between  $\rho_{11}$  and the other two diagonal components (which are nearly equal); and the differences between  $\rho_{12}$  and  $\rho_{21}$ .

#### IV. GENERALIZED LANGEVIN MODEL

In PDF methods, the stochastic Lagrangian model for velocity that is employed is the generalized Langevin model (GLM).<sup>11,12,7</sup> Applied to homogeneous turbulence, the model for  $\mathbf{u}(t)$  is

$$d\mathbf{u}_i = -\frac{\partial \langle U_i \rangle}{\partial x_j} u_j dt + G_{ij} u_j dt + (C_0 \varepsilon)^{1/2} dW_i, \quad (34)$$

where the constant  $C_0$  is generally ascribed the value 2.1. The coefficient  $G_{ij}$  can depend on  $\langle u_i u_j \rangle$ ,  $\varepsilon$  and  $\partial \langle U_i \rangle / \partial x_j$ : two particular specifications of  $G_{ij}$  are considered below.

The transformation of Eq. (34) to an SDE for  $\hat{\mathbf{u}}(\hat{t})$  results in the general stochastic model, Eq. (19), with coefficients

$$A_{ij} = \frac{1}{2} \left( \frac{\mathcal{P}}{\varepsilon} - 1 \right) \delta_{ij} + \frac{k}{\varepsilon} \frac{\partial \langle U_i \rangle}{\partial x_j} - \frac{k}{\varepsilon} G_{ij}, \quad (35)$$

and

$$B_{ij} = C_0^{1/2} \delta_{ij}. \quad (36)$$

Equation (35) can be rearranged to yield the value of  $(k/\varepsilon)G_{ij}$  implied by the DNS:

$$\frac{k}{\varepsilon} \mathbf{G} = \begin{bmatrix} -2.18 & 3.59 & 0 \\ -0.65 & -4.63 & 0 \\ 0 & 0 & -3.95 \end{bmatrix}. \quad (37)$$

Since  $\mathbf{B}$  is found to be anisotropic—as discussed further in the next subsection—no choice of  $C_0$  in Eq. (36) yields the correct diffusion coefficient. Nevertheless, the magnitude of the diffusion is characterized by

$$\hat{C}_0 \equiv \frac{1}{3} \text{trace}(\mathbf{B}^2), \quad (38)$$

the value of which deduced from the DNS is  $\hat{C}_0 = 4.3$ . By comparison, the standard model Eq. (36) yields  $\hat{C}_0 = C_0 = 2.1$ .

#### A. Anisotropy of the diffusion coefficient

The GLM, and also dispersion models, take the diffusion coefficient  $\mathbf{B}$  to be isotropic, Eq. (36). The reason generally advanced for this specification is consistency with the Kolmogorov hypotheses. For (dimensional) time intervals  $s$  in the inertial subrange,  $\tau_\eta \ll s \ll k/\varepsilon$  (where  $\tau_\eta$  is the Kolmogorov timescale), the Kolmogorov hypotheses predict that the second-order Lagrangian structure function is isotropic and linear in  $s$ , i.e.,

$$\langle [u_i(t+s) - u_i(t)][u_j(t+s) - u_j(t)] \rangle = C_0 \varepsilon s \delta_{ij}, \quad (39)$$

where  $C_0$  is a Kolmogorov constant. The GLM yields precisely this result if  $C_0$  is taken to be  $C_0$ .

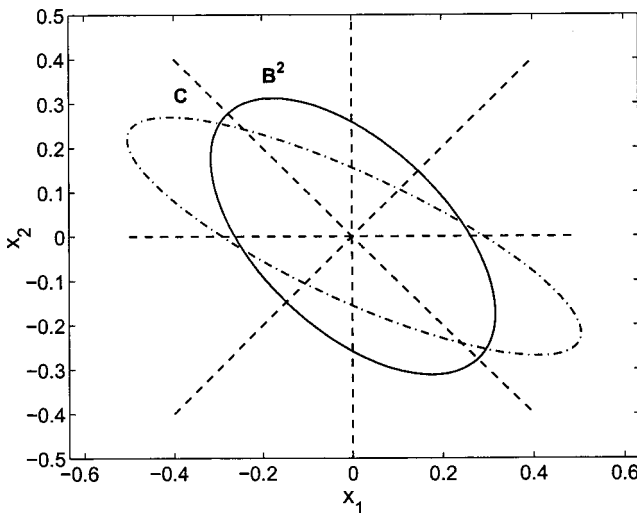


FIG. 4. The scaled tensors  $\mathbf{B}^2$  and  $\mathbf{C}$  shows as ellipses in the  $x_1-x_2$  plane. The dot-dashed line is  $x_i x_j C_{ij}^{-2} = (C_{ii})^{-2}$ , and the solid line is the corresponding ellipse for  $\mathbf{B}^2$ . Shown for reference are dashed lines at  $0^\circ$ ,  $45^\circ$ ,  $90^\circ$ , and  $135^\circ$ .

However, the value of  $\mathbf{B}^2$  deduced from the DNS is decidedly anisotropic: the eigenvalues of  $\mathbf{B}^2$  (which are all equal to  $C_0=2.1$  in the GLM) are found to be 2.69, 5.06, and 5.14. It is possible that this anisotropy is a Reynolds-number effect, which vanishes at sufficiently high Reynolds number. This possibility could be investigated through DNS at different Reynolds numbers.

It is also possible that the anisotropy in the deduced value of  $\mathbf{B}^2$  persists at high Reynolds numbers, not because the Kolmogorov hypothesis [Eq. (39)] is incorrect, but because the stochastic Lagrangian model, Eq. (19), is too simple to represent the multi-timescale aspects of anisotropic turbulence.

Given the observation that  $\mathbf{B}^2$  is anisotropic, it is natural to consider modifications to the GLM to incorporate such anisotropy. The natural way to introduce anisotropy in the model is to make the diffusion coefficient dependent on the normalized Reynolds stresses  $\mathbf{C}$ . But any such model implies that the principal axes of  $\mathbf{B}^2$  and  $\mathbf{C}$  are aligned, which is not supported by the data. Figure 4 shows the ellipses in the  $x_1-x_2$  plane corresponding to the tensors  $\mathbf{B}^2$  and  $\mathbf{C}$ . The misalignment of the principal axes is evident. In fact, to within  $1^\circ$ , the minor axis of  $\mathbf{B}^2$  is aligned with the major axis of the mean rate-of-stain tensor  $\mathbf{S}$  (i.e., the  $45^\circ$  line  $x_2=x_1$ ). Hence an anisotropic model for  $\mathbf{B}^2$  could be constructed based on  $\mathbf{S}$  that is consistent with the DNS data. More data—from different flows and at different Reynolds numbers—are needed before an anisotropic model for  $\mathbf{B}^2$  of any generality can be constructed.

## B. Simplified Langevin model

In this and the next subsection we examine two specific forms of the generalized Langevin model, corresponding to particular specifications of  $G_{ij}$ .

For the simplified Langevin model (SLM) considered here, the specification is

TABLE I. Values of the mean timescale  $T \equiv \frac{1}{3} \text{trace}(\mathbf{T})$ , the normalized Reynolds stress  $C_{ij}$ , and the turbulence-to-shear timescale ratio  $Sk/\varepsilon$  from the DNS of Sawford and Yeung (Ref. 5) and from SLM and LIPM for different values of  $C_0$  and  $\alpha_2$ .

	DNS	SLM	SLM	LIPM	LIPM
$C_0$	-	2.1	3.4	2.1	4.4
$\alpha_2$	-	-	-	3.5	11.9
$T$	0.30	0.43	0.30	0.63	0.30
$C_{11}$	0.96	1.10	0.98	1.02	1.02
$C_{22}$	0.43	0.45	0.51	0.49	0.49
$C_{33}$	0.61	0.51	0.51	0.49	0.49
$C_{12}$	-0.32	-0.39	-0.34	-0.36	-0.36
$Sk/\varepsilon$	4.83	4.02	4.47	4.28	4.28

$$G_{ij} = -\left(\frac{1}{2} + \frac{3}{4} C_0\right) \frac{\varepsilon}{k} \delta_{ij}, \quad (40)$$

so that the matrix  $\mathbf{A}$  [Eq. (35)] is

$$\mathbf{A} = \begin{bmatrix} \lambda & \sigma & 0 \\ 0 & \lambda & 0 \\ 0 & 0 & \lambda \end{bmatrix}, \quad (41)$$

with

$$\lambda = \frac{1}{2} \frac{\mathcal{P}}{\varepsilon} + \frac{3}{4} C_0, \quad (42)$$

and

$$\sigma = Sk/\varepsilon.$$

Evidently all three eigenvalues of  $\mathbf{A}$  are equal to  $\lambda$ , and the eigenvectors are not independent—two are equal to  $[1 \ 0 \ 0]^T$ . Consequently, the autocovariance  $\hat{\mathbf{R}}(s)$  is not given by Eq. (25), but instead the solution to Eq. (21) is

$$\hat{\mathbf{R}}(s) = e^{-\lambda s} \begin{bmatrix} C_{11} - \sigma s C_{12} & C_{12} & 0 \\ C_{21} - \sigma s C_{22} & C_{22} & 0 \\ 0 & 0 & C_{33} \end{bmatrix}. \quad (43)$$

Given a specified value of  $C_0$  and the DNS value of  $\mathcal{P}/\varepsilon$ , Eq. (31) can be solved to determine the normalized Reynolds stresses  $\mathbf{C}$  given by SLM in homogeneous turbulent shear flow, and then the autocovariances can be evaluated from Eq. (43). We consider two values of  $C_0$ : the standard value  $C_0=2.1$ ; and the value  $C_0=3.4$  for which the SLM timescale  $\lambda^{-1}$  matches the average DNS timescale  $T \equiv \frac{1}{3} \text{trace}(\mathbf{T})$ . The values of  $\mathbf{C}$  obtained are shown in Table I.

The autocorrelations  $\rho_{ij}(s)$  obtained with  $C_0=3.4$  are compared to the DNS data in Fig. 5. As expected, the agreement is much better with the timescales matched ( $C_0=3.4$ ) than otherwise ( $C_0=2.1$ , not shown). The model correctly predicts the equality of  $\rho_{22}$  and  $\rho_{33}$  and their distinction from  $\rho_{11}$ , but the quantitative agreement is noticeably poorer than in Fig. 3.

The model predicts a more substantial difference between  $\rho_{12}(s)$  and  $\rho_{21}(s)$  than is evident in the DNS—a behavior which is easily understood. The only off-diagonal term [ $\sigma$  in Eq. (41)] enters the SDE for velocity as

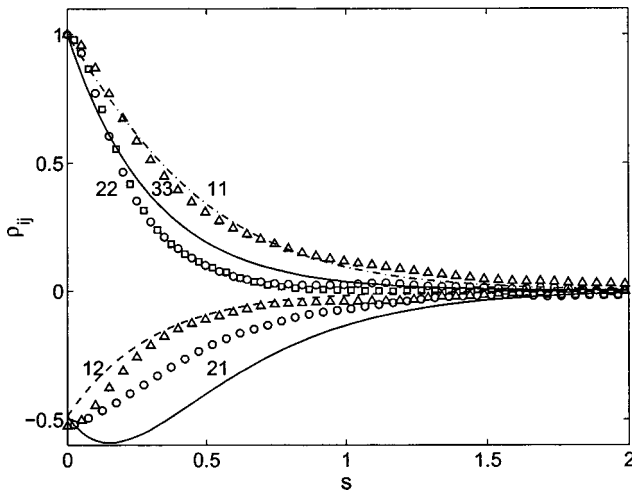


FIG. 5. Comparison of autocorrelation functions  $\rho_{ij}(s)$ , Eq. (14), from DNS (symbols) and from SLM with  $C_0=3.4$ . (For SLM,  $\rho_{22}=\rho_{33}$ .)

$$d\hat{u}_1 = -\frac{Sk}{\varepsilon} \hat{u}_2 d\hat{t} \dots \quad (44)$$

Thus large positive (or negative) values of  $\hat{u}_2$  tend to lead to large negative (or positive) values of  $\hat{u}_1$  after a time lag. Thus the peak correlation  $|\langle \hat{u}_2(\hat{t}) \hat{u}_1(\hat{t}+s) \rangle|$ —or equivalently the minimum of  $\rho_{21}(s)$ —occurs for a positive value of  $s$ . The model overestimates this effect, because it takes no account of rapid pressure fluctuations which tend to counteract the effects of mean shear.

### C. Lagrangian isotropization of production model (LIPM)

The LIPM<sup>14,7</sup> corresponds closely to the Launder, Reece, and Rodi<sup>16</sup> Reynolds-stress model. Using standard values for the model constants  $\beta_{1-3}$  and  $\gamma_{1-6}$ , the LIPM equation for  $\mathbf{G}$  is

$$\begin{aligned} \frac{k}{\varepsilon} \mathbf{G} &= \alpha_1 \mathbf{I} + \alpha_2 (\mathbf{b} - 3\mathbf{b}^2) \\ &+ \frac{Sk}{\varepsilon} \begin{bmatrix} -\frac{3}{5}b_{12} & \frac{4}{5} + \frac{3}{5}b_{11} & 0 \\ -\frac{1}{5} - \frac{3}{5}b_{22} & \frac{3}{5}b_{12} & 0 \\ 0 & 0 & 0 \end{bmatrix}, \end{aligned} \quad (45)$$

where  $\mathbf{b}$  is the anisotropy tensor

$$\mathbf{b} = \frac{1}{2} \mathbf{C} - \frac{1}{3} \mathbf{I}, \quad (46)$$

the standard value of the constant  $\alpha_2$  is  $\alpha_2=3.5$ , and the coefficient  $\alpha_1$  is given by

$$\alpha_1 = -\left(\frac{1}{2} + \frac{3}{4}C_0\right) + \frac{3}{10} \frac{\mathcal{P}}{\varepsilon} + 3\alpha_2 \text{trace}(\mathbf{b}^3). \quad (47)$$

With the standard value  $C_0=2.1$ , the model yields reasonable values of the normalized Reynolds stresses, but the average time scale  $T \equiv \frac{1}{3} \text{trace}(\mathbf{T})$  is more than twice the

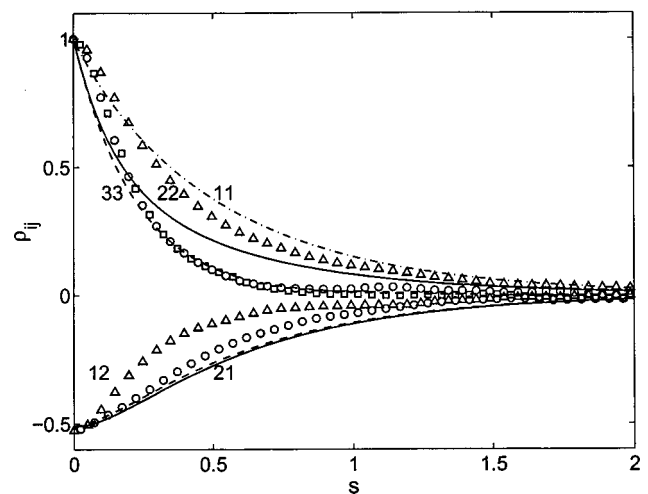


FIG. 6. Comparison of autocorrelation functions  $\rho_{ij}(s)$ , Eq. (14), from DNS (symbols) and from LIPM with  $C_0=4.4$  and  $\alpha_2=11.9$  (lines). Dashed lines,  $\rho_{12}$  and  $\rho_{33}$ ; solid lines,  $\rho_{21}$  and  $\rho_{22}$ .

DNS value; see Table I. As a consequence, the model (with  $C_0=2.1$ ) produces autocorrelations  $\rho_{ij}(s)$  (not shown) in very poor agreement with the DNS data.

To provide a more meaningful comparison, the constants  $C_0$  and  $\alpha_2$  are adjusted to match the average timescale, while leaving the normalized Reynolds stresses the same. The autocorrelations given by LIPM with these values ( $C_0=4.4$ ,  $\alpha_2=11.9$ ) are compared to the DNS data in Fig. 6. The agreement is quite poor. Except at small times,  $\rho_{22}(s)$  is incorrectly predicted to be larger than  $\rho_{33}(s)$ ; and evidently the effect of the rapid pressure is overpredicted as there is little difference between  $\rho_{12}(s)$  and  $\rho_{21}(s)$ .

This last point can be seen directly in the matrix  $\mathbf{A}$ , which for LIPM is

$$\mathbf{A} = \begin{bmatrix} 2.86 & 1.99 & 0 \\ 2.21 & 6.11 & 0 \\ 0 & 0 & 4.48 \end{bmatrix}. \quad (48)$$

The direct effect of shear appears in the 1–2 component, and in SLM the 2–1 component is zero. In  $\mathbf{A}$  deduced from the DNS data [Eq. (32)],  $A_{21}$  is about half of  $A_{12}$ ; but for LIPM  $A_{21}$  exceeds  $A_{12}$ .

### V. CONCLUSIONS

As previously observed by Sawford and Yeung<sup>4,5</sup> in the context of turbulent dispersion, Lagrangian data from DNS of homogeneous turbulence is valuable in the development and testing of stochastic Lagrangian models. After an initial transient, homogeneous turbulent shear becomes (approximately) self-similar, so that the appropriately scaled Lagrangian velocity fluctuation  $\hat{\mathbf{u}}(\hat{t})$  becomes a statistically stationary random process.

The stochastic Lagrangian model considered for  $\hat{\mathbf{u}}(\hat{t})$  is the diffusion process Eq. (19) in which the drift coefficient depends linearly on  $\hat{\mathbf{u}}(\hat{t})$  through the drift matrix  $\mathbf{A}$ , and the (anisotropic) diffusion coefficient  $\mathbf{B}$  is constant. An analysis of this model shows that there is a unique specification of  $\mathbf{A}$

and  $\mathbf{B}$  [Eq. (30) and Eq. (31)] such that the covariance matrix  $\mathbf{C}$  and the timescale matrix  $\mathbf{T}$  match those obtained from DNS. The autocorrelation functions predicted by the model are in good agreement with the DNS data (except at small times). The model for  $\hat{\mathbf{u}}(\hat{t})$  is a continuous, Gaussian, Markov process; and it is a significant conclusion that such a simple process provides a good model for the Lagrangian velocity in homogeneous turbulent shear flow. (It is known that the one-point one-time joint PDF of velocity is jointly normal<sup>1</sup> in this flow.)

Contrary to conventional modelling assumptions, it is found that the diffusion coefficient  $\mathbf{B}$  is significantly anisotropic. Whether or not this is a low Reynolds-number effect is an important question which can be addressed in future DNS studies.

The magnitude of the diffusion coefficient can be characterized by  $\hat{C}_0 = \frac{1}{3} \text{trace}(\mathbf{B}^2)$  and the value deduced from the DNS data is  $\hat{C}_0 = 4.3$ . This is substantially larger than the corresponding value  $C_0 = 2.1$  normally used in PDF models.

There is evidence that the appropriate value of  $C_0$  depends on Reynolds number.<sup>13,10</sup> In the DNS, the Taylor-scale Reynolds number based on  $x_1$ -direction statistics increases from  $R_\lambda \approx 40$  to  $R_\lambda \approx 110$  during the course of the simulation. Sawford and Yeung<sup>5</sup> provide an empirical expression for  $C_0$  as a function of  $R_\lambda$ , which increase from  $C_0 = 3.7$  at  $R_\lambda = 40$  to  $C_0 = 5.4$  at  $R_\lambda = 110$ . The value  $C_0 = 4.3$  deduced from the DNS lies within this range, but Reynolds-number effects are not addressed here.

The autocorrelation functions predicted by two generalized Langevin models are compared to the DNS data in Figs. 5 and 6. In the simplified Langevin model (SLM), no account is taken of the rapid pressure fluctuations, and as a consequence the difference between  $\rho_{12}(s)$  and  $\rho_{21}(s)$  is overpredicted. The Lagrangian IP model (LIPM)—which includes a model for the rapid pressure—yields autocorrelations in poor agreement with the DNS data.

In the specification of both the drift and diffusion coefficients, there is clearly scope for considerable improvement in generalized Langevin models.

## ACKNOWLEDGMENTS

The author is grateful to Professor P. K. Yeung and Dr. B. L. Sawford for making available their DNS data; to Professor D. L. Koch and J. Chen for discussions on the solution of the stochastic model equations; and to Professor R. O. Fox for clarifying the necessary conditions for the satisfaction of Eq. (23). This work was supported by Air Force Office of Scientific Research Grant No. F49620-00-1-0171.

- <sup>1</sup>S. Tavoularis and S. Corrsin, "Experiments in nearly homogeneous turbulent shear flow with a uniform mean temperature gradient. Part 1," *J. Fluid Mech.* **104**, 311 (1981).
- <sup>2</sup>M. M. Rogers and P. Moin, "The structure of the vorticity field in homogeneous turbulent flows," *J. Fluid Mech.* **176**, 33 (1987).
- <sup>3</sup>P. Shen and P. K. Yeung, "Fluid particle dispersion in homogeneous turbulent shear," *Phys. Fluids* **9**, 3472 (1997).
- <sup>4</sup>B. L. Sawford and P. K. Yeung, "Eulerian acceleration statistics as a discriminator between Lagrangian stochastic models in uniform shear flow," *Phys. Fluids* **12**, 2033 (2000).
- <sup>5</sup>B. L. Sawford and P. K. Yeung, "Lagrangian statistics in uniform shear flow: Direct numerical simulation and Lagrangian stochastic models," *Phys. Fluids* **13**, 2627 (2001).
- <sup>6</sup>S. B. Pope, "Lagrangian PDF methods for turbulent flows," *Annu. Rev. Fluid Mech.* **26**, 23 (1994).
- <sup>7</sup>S. B. Pope, *Turbulent Flows* (Cambridge University Press, Cambridge, 2000).
- <sup>8</sup>G. I. Taylor, "Diffusion by continuous movements," *Proc. London Math. Soc.* **20**, 196 (1921).
- <sup>9</sup>D. J. Thomson, "Criteria for the selection of stochastic models of particle trajectories in turbulent flows," *J. Fluid Mech.* **180**, 529 (1987).
- <sup>10</sup>B. L. Sawford, "Rotation in Lagrangian stochastic models of turbulent dispersion," *Boundary-Layer Meteorol.* **93**, 411 (1999).
- <sup>11</sup>S. B. Pope, "A Lagrangian two-time probability density function equation for inhomogeneous turbulent flows," *Phys. Fluids* **26**, 3448 (1983).
- <sup>12</sup>D. C. Haworth and S. B. Pope, "A generalized Langevin model for turbulent flows," *Phys. Fluids* **29**, 387 (1986).
- <sup>13</sup>P. K. Yeung and S. B. Pope, "Lagrangian statistics from direct numerical simulations of isotropic turbulence," *J. Fluid Mech.* **207**, 531 (1989).
- <sup>14</sup>S. B. Pope, "On the relationship between stochastic Lagrangian models of turbulence and second-moment closures," *Phys. Fluids* **6**, 973 (1994).
- <sup>15</sup>C. W. Gardiner, *Handbook of Stochastic Methods for Physics, Chemistry and the Natural Sciences*, 2nd ed. (Springer-Verlag, Berlin, 1985).
- <sup>16</sup>B. E. Launder, G. J. Reece, and W. Rodi, "Progress in the development of a Reynolds-stress turbulence closure," *J. Fluid Mech.* **68**, 537 (1975).